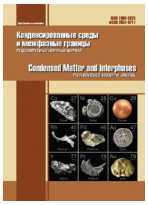

ISSN 1606-867X (Print)
ISSN 2687-0711 (Online)
Condensed Matter and Interphases
Kondensirovannye Sredy i Mezhfaznye Granitsy
https://journals.vsu.ru/kcmf/

Original articles

Research article
https://doi.org/10.17308/kcmf.2022.24/9852

Synthesis of magnetic chromium substituted cobalt ferrite $Co(Cr_xFe_{1-x})_2O_4$ adsorbents for phosphate removal

Qui Anh Tran[1, 2], Nhat Linh Tran[1,2], Dang Khoa Nguyen Anh[1, 2], Quynh Nhu Le Thi[1, 2], The Luan Nguyen[1,2], Huu Thinh Pham Nguyen[1,2], Anh Tien Nguyen[3], Quoc Thiet Nguyen[4], Tien Khoa Le[1,2] ✉

[1]Faculty of Chemistry, University of Science, Ho Chi Minh city, Vietnam

[2]Faculty of Chemistry, University of Science, Vietnam National University, Ho Chi Minh City, Vietnam

[3] Faculty of Chemistry, Ho Chi Minh City University of Education, Ho Chi Minh City, Vietnam

[4]Institute of Applied Materials Science, Vietnam Academy of Science and Technology, 1B TL29 District 12, Ho Chi Minh City, Vietnam

Abstract

In this work, we aimed to prepare chromium substituted cobalt ferrite $Co(Cr_xFe_{1-x})_2O_4$ powders by a simple coprecipitation-annealing method with different Cr contents to create novel magnetic adsorbents for the removal of phosphate ions from water. The effects of Cr substitution on the crystal structure, phase composition, morphology, surface atomic composition, surface area and magnetic properties of our adsorbents were investigated by X-ray diffraction, scanning electron microscopy, energy-dispersive X-ray spectroscopy, Brunauer-Emmett-Teller nitrogen adsorption-desorption and vibrating sample magnetometry. According to the results, all our $Co(Cr_xFe_{1-x})_2O_4$ samples exhibited higher phosphate adsorption than $CoFe_2O_4$ powder but their magnetic properties were reduced for increasing Cr substitution. Among them, the $Co(Cr_{0.25}Fe_{0.75})_2O_4$ sample was found to be the most promising material since its magnetic properties are still high to allow it to be easily separated from the solution and its maximum P adsorption capacity (according to the Langmuir model) was estimated to be 4.84 times higher than $CoFe_2O_4$, which can be attributed to the presence of Cr^{3+} ions on the surface and the enhanced surface specific area of this substituted sample. Moreover, the adsorption data of $Co(Cr_{0.25}Fe_{0.75})_2O_4$ sample also fitted well to the pseudo second order kinetic model, revealing the adsorption rate constant of 0.87 $mgP^{-1}s^{-1}$, two times superior to $CoFe_2O_4$.

Keywords: Chromium substitution; Cobalt ferrite; Phosphate removal; Magnetic adsorbent; Surface Cr^{3+} content

For citation: Tran Q. A., Tran N. L., Nguyen A. D. K., Le T. Q. N., Nguyen L. T., Nguyen H. T. P., Nguyen A. T., Nguyen T., Q., Le T. K. Synthesis of magnetic chromium substituted cobalt ferrite Co(CrxFe1–x)2O4 adsorbents for phosphate removal. *Condensed Matter and Interphases*. 2022;24(3): 306–314. https://doi.org/10.17308/kcmf.2022.24/9852

Для цитирования Чан К. А., Чан Н. Л., Нгуен А. Д. К., Ле Т. К. Н., Нгуен Л. Т., Нгуен Ч. Т. Ф., Нгуен А. Т., Нгуен Т. К., Ле Т. К. Синтез магнитных адсорбентов хромзамещенных ферритов кобальта $Co(Cr_xFe_{1-x})_2O_4$ для удаления фосфатов. *Конденсированные среды и межфазные границы*.2022;24(3): 306–314. https://doi.org/10.17308/kcmf.2022.24/9852

✉ Tien Khoa Le, e-mail: ltkhoa@hcmus.edu.vn

1. Introduction

For a long time, the presence of phosphate ions in wastewater has been largely considered as the main factor causing eutrophication [1, 2], a phenomenon characterized by the excessive algal growth, which can lead to numerous ecological disturbances, such as the bloom of cyanobacteria, the impairment of water quality and the hypoxia problem [3]. Hence, removing phosphate ions from wastewater before discharge is always a crucial task of environmental control strategies. In the literature, among different approaches including adsorption, chemical precipitation and biological removal, adsorption is found to be an economical, simple and effective method for the removal of phosphate ions in low concentration without formation of chemical waste sludge [4, 5]. However, most of phosphate adsorbent materials such as fly ash [6], porous metal oxides [7], metal organic frameworks [8] and layered double hydroxides [9] were developed in the form of fine powder which has the high suspendability in water and thus is very difficult to be separated from water bodies after treatment.

To address this problem, magnetically separable adsorbents based on ferrite materials were introduced. In fact, owing to their ferromagnetic properties, ferrite oxides have been extensively studied for various applications, including electromagnetic devices [10] magnetorheological fluids [11] and magnetic Fenton catalysts [12]. Hence, some recent studies have suggested to prepare magnetic phosphate adsorbents possessing the core-shell structure with ferrite particles as a magnetic core. For example, Lai et al. successfully prepared magnetic Fe_3O_4@SiO_2 core-shell nanoparticles functionalized by hydrous lanthanum oxide, which exhibited both high phosphate adsorption and good magnetic properties, facilitating the separation and recovery of core-shell materials [13]. Likewise, Lin et al. also reported the effective phosphate adsorption using Fe_3O_4@MgAl-LDH@$La(OH)_3$ composites with a hierarchical core-shell structure [14]. Thanks to their magnetite core, more than 79% of composite powders can be recovered from solution by a magnet [14]. However, the core-shell adsorbents were usually prepared by complicated procedures which increases their production cost. Besides, during phosphate removal, the shell component can be separated from the inner magnetic core since the bonding strength between the shell and the core is still a question mark.

Therefore, in this work, we proposed to developed novel magnetic phosphate adsorbents without core-shell structure, based on chromium substituted cobalt ferrite $Co(Cr_xFe_{1-x})_2O_4$ powders. These samples were prepared by a simple coprecipitation-annealing method with different Cr contents and then characterized in terms of phase composition, surface atomic composition, morphology, surface area and magnetic parameters. Their maximum P adsorption capacity and their adsorption kinetics for phosphate removal were also investigated.

2. Experimental

2.1. Synthesis of magnetic adsorbents

For the synthesis of $Co(Cr_xFe_{1-x})_2O_4$ with x = 0, 0.25, 0.50 and 0.75, the starting precursors including $CoCl_6 \cdot 6H_2O$, $Fe(NO_3)_3 \cdot 9H_2O$ and $Cr(NO_3)_3 \cdot 9H_2O$ (> 98%, purchased from Sigma Aldrich) were separately dissolved in distilled water and then mixed together following the desired molar Co/Cr/Fe ratios. Subsequently, NaOH solution (4.0 mol/L^{-1}) was slowly added to the solution containing Co^{2+}, Fe^{3+} and Cr^{3+} under regular stirring until pH 7. This solution was heated and maintained at 90 °C for 2 hours. After that, the precipitates were filtered, washed with distilled water, dried at 150 °C for 8 hours and ground into a fine powder. The powders were annealed at 700 °C for 4 hours. Next, the products were washed with distilled water, separated from water by a magnet and finally dried again at 150 °C for 1 hour to obtain $Co(Cr_xFe_{1-x})_2O_4$ samples.

2.2. Material characterization

The magnetic measurement for $Co(Cr_xFe_{1-x})_2O_4$ adsorbents was carried out at room temperature by using a vibrating sample magnetometer PPMS6000 (Quantum Design). Their crystal structure and phase composition were investigated by powder X ray diffraction (XRD) using a BRUKER-Binary V3 X-ray diffractometer with Cu$K\alpha$ radiation (λ = 1.5406 Å) in the 2θ range of 10–80° (0.02° per step). The morphology of these samples was observed by a field emission

scanning electron microscope (FE-SEM) HITACHI S-48000 under an accelerating voltage of 10 kV. The energy-dispersive X-ray spectroscopy (EDS) analysis was also conducted using HITACHI S-4800 microscope to determine the surface atomic composition of our adsorbents. Moreover, their specific surface area was measured by using the Brunauer-Emmett-Teller (BET) method with N_2 adsorption-desorption isotherms recorded at 77 K on a NOVA 1000e analyzer (Quantachrome Instruments).

2.3. Preliminary tests for phosphate adsorption

The preliminary adsorption tests of our $Co(Cr_xFe_{1-x})_2O_4$ adsorbents toward phosphate ions were performed by dispersing adsorbent powder (0.20 g) in the glass beaker containing 100 mL of KH_2PO_4 solution (2 mgP/L^{-1}) without artificial pH adjustment. The beaker was sealed and placed in a circulation system of water to maintain the temperature at about 30 °C. The suspension was constantly stirred for 24 hours. Then, the magnetic adsorbent was separated from the phosphate solution by using a magnet and the phosphate concentration of this solution was determined by the molybdenum blue colorimetric method [15] using a Helios Omega UV – VIS spectrophotometer (Thermo Fisher Scientific, USA) to measure the absorbance at 880 nm. The phosphate removal yield (%) and the phosphate uptake capacity at equilibrium (q_e, mgP.g^{-1}) of $Co(Cr_xFe_{1-x})_2O_4$ samples were calculated by the following equations (Eq. 1 and 2):

$$\text{Yield (\%)} = \frac{C_0 - C_f}{C_0} \times 100, \quad (1)$$

$$q_e = \frac{(C_0 - C_f)V}{m_{adsorbent}}, \quad (2)$$

where C_0 and C_f are the initial and final concentration of phosphate solution (mgP/L^{-1}), V is the solution volume (L) and $m_{adsorbent}$ is the mass of adsorbent (g).

2.4. Adsorption isotherms

In order to determine the maximum phosphate adsorption capacity of our samples, the study of adsorption isotherms was conducted by adding 0.02 g of samples into 100 mL of KH_2PO_4 solutions with different phosphate concentrations (2–100 mgP.L^{-1}). These suspensions were regularly stirred at about 30°C (by using a circulation system of water) for 24 hours. After that, the equilibrium adsorption capacity for phosphate of our samples was calculated according to Eq. 2. These isotherm data were consequently analyzed using two adsorption Langmuir and the Freundlich models which can be expressed by the Eq. 3 and Eq. 4, respectively:

$$\frac{C_e}{q_e} = \frac{C_e}{C_0} + \frac{1}{K_L \times q_m}, \quad (3)$$

$$\ln q_e = \ln K_F + \frac{1}{n} \times \ln C_e, \quad (4)$$

where C_e (mgP/L^{-1}) and q_e (mgP/g^{-1}) are the phosphate concentration and the phosphate adsorption capacity of $Co(Cr_xFe_{1-x})_2O_4$ at equilibrium, respectively, q_m is the maximum phosphate adsorption capacity (mgP/g^{-1}), K_L is a Langmuir constant associated with the affinity of binding sites (L/mg^{-1}), K_F is a Freundlich constant related to the adsorption capacity (mgP/g^{-1}) and n is the constant related to the adsorption density.

2.5. Adsorption kinetics

In order to investigate the phosphate adsorption kinetics of $Co(Cr_xFe_{1-x})_2O_4$ samples, the adsorption tests were carried out in the same way of our isotherm study except the fact that the initial phosphate concentration was fixed at 2 mgP/L^{-1}. At given time intervals, aliquots of solution were collected, followed by the separation of magnetic adsorbents by a magnet and the concentrations of remaining phosphate ions were determined. Then, two kinetic models, the pseudo first-order (Eq. 5) and the pseudo second-order (Eq. 6) were used to fit the adsorption data of our samples:

$$\log(q_e - q_t) = \log q_e - \frac{k_1 t}{2.303}, \quad (5)$$

$$\frac{t}{q_t} = \frac{1}{k_2 q_e^2} + \frac{t}{q_e}, \quad (6)$$

where q_e (mgP/g^{-1}) and q_t (mgP/g^{-1}) are the phosphate adsorption capacity of $Co(Cr_xFe_{1-x})_2O_4$ at equilibrium and time t (min), k_1 (min^{-1}) and k_2 (g/mgP^{-1}· min^{-1}) are the adsorption rate constants corresponding to the pseudo first-order and pseudo second-order kinetic models, respectively.

3. Results and discussion

3.1. Preliminary tests for phosphate adsorption

The phosphate removal yield and the phosphate uptake capacity at equilibrium of $Co(Cr_xFe_{1-x})_2O_4$ samples measured in our preliminary tests after 24 hours were presented in Table 1. Without Cr substitution, our $CoFe_2O_4$ sample only exhibited a low phosphate adsorption with the removal yield of 29.45 % and the uptake capacity of 0.31 mgP/g^{-1}. When Cr^{3+} ions were introduced into $Co(Cr_xFe_{1-x})_2O_4$ samples, the phosphate adsorption was greatly improved, indicating that the presence of Cr^{3+} ions may act as new and efficient adsorption sites toward phosphate ions. With x = 0.25, the phosphate removal yield and the phosphate uptake capacity reached 58.91% and 0.61 mgP/g^{-1}, respectively, which are about two times higher than $CoFe_2O_4$. However, when the substituent Cr content further increased (x = 0.50, 0.75), the adsorption capacity and the removal yield were only slightly enhanced, suggesting that the increase of Cr content did not strongly affect the adsorption capacity of $Co(Cr_xFe_{1-x})_2O_4$ samples.

3.2. Magnetic properties

Fig. 1 and Table 2 display the magnetic hysteresis loops and the magnetic parameters of our $Co(Cr_xFe_{1-x})_2O_4$ samples, respectively. Generally, magnetic adsorbent powders usually need high saturation magnetization (M_S) to be easily attracted by using an external magnetic field and low coercivity (H_C) to be easily redispersed for the next runs. It was observed that $CoFe_2O_4$ sample presented the hard ferromagnetic behavior at room temperature with the saturation magnetization of 65.90 emu/g^{-1} and the coercivity of 646.32 Oe. For $Co(Cr_{0.25}Fe_{0.75})_2O_4$ sample, these both magnetic parameters were clearly declined (M_S = 41.25 emu/g^{-1} and H_C = 181.60 Oe). This evolution can be attributed to the replacement of Fe^{3+} ions by Cr^{3+} ions in the oxide lattice. In fact, the magnetic moment of Cr^{3+} ion (3 μB) is lower than that of Fe^{3+} ion (5 μB) [16]. Hence, when an amount of Fe^{3+} ions at the octahedral sites were replaced by Cr^{3+} ions, the A-B super exchange interaction was declined, which causes the decrease in saturation magnetization of chromium substituted materials. Moreover, the reduction of magnetization could also turn our samples into soft magnetic materials, causing the decrease in coercivity [17]. These results are found to be in good agreement with previous works [17–19]. Fortunately, the saturation magnetization of $Co(Cr_{0.25}Fe_{0.75})_2O_4$ is still high enough to allow the quick separation from the solution by a

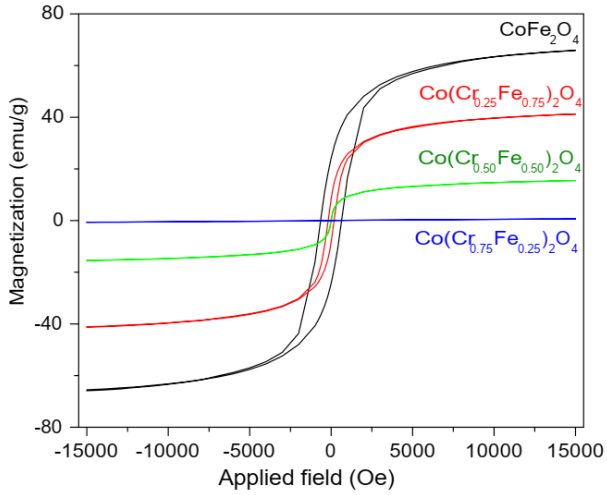

Fig. 1. Magnetic hysteresis loops of $CoFe_2O_4$, $Co(Cr_{0.25}Fe_{0.75})_2O_4$, $Co(Cr_{0.50}Fe_{0.50})_2O_4$ and $Co(Cr_{0.75}Fe_{0.25})_2O_4$ samples

Table 1. Phosphate removal yield (Y %) and phosphate uptake capacity (q_e) of $CoFe_2O_4$, $Co(Cr_{0.25}Fe_{0.75})_2O_4$, $Co(Cr_{0.50}Fe_{0.50})_2O_4$ and $Co(Cr_{0.75}Fe_{0.25})_2O_4$ in our preliminary tests after 24 hours

Samples	$CoFe_2O_4$	$Co(Cr_{0.25}Fe_{0.75})_2O_4$	$Co(Cr_{0.50}Fe_{0.50})_2O_4$	$Co(Cr_{0.75}Fe_{0.25})_2O_4$
Y %	29.45	58.91	58.22	66.36
q_e (mgP g^{-1})	0.31	0.61	0.60	0.68

Table 2. Magnetic parameters of $CoFe_2O_4$, $Co(Cr_{0.25}Fe_{0.75})_2O_4$, $Co(Cr_{0.50}Fe_{0.50})_2O_4$, and $Co(Cr_{0.75}Fe_{0.25})_2O_4$ samples

Samples	$CoFe_2O_4$	$Co(Cr_{0.25}Fe_{0.75})_2O_4$	$Co(Cr_{0.50}Fe_{0.50})_2O_4$	$Co(Cr_{0.75}Fe_{0.25})_2O_4$
M_S (emu g^{-1})	65.903	41.251	15.492	0.671
H_C (Oe)	646.320	181.60	13.54	104.60

magnet. However, for $Co(Cr_{0.50}Fe_{0.50})_2O_4$ and $Co(Cr_{0.75}Fe_{0.25})_2O_4$ samples, the M_S value was dramatically declined, making it very difficult to separate these samples by a magnet. Therefore, from the results of preliminary adsorption tests and magnetic analysis, the $Co(Cr_{0.25}Fe_{0.75})_2O_4$ sample can be considered as the most promising magnetic adsorbent among our chromium substituted materials.

3.3. Crystal structure and atomic composition

Figure 2 displays XRD patterns of our $CoFe_2O_4$ and $Co(Cr_{0.25}Fe_{0.75})_2O_4$ samples. The pattern of $CoFe_2O_4$ sample shows the pure phase of cubic spinel cobalt ferrite (space group Fd3m, JCPDS No.22-1086), identified by the XRD peaks at 18.33, 29.91, 30.70, 34.68, 36.01, 43.97, 58.09 and 62.15°. From this pattern, the cell parameter of cubic spinel lattice was found to be 8.375 Å. When Fe^{3+} ions were replaced by Cr^{3+} ions with x = 0.25, no additional phase and no evolution of cell parameters have been detected in the XRD pattern, indicating that the chromium substitution at the level of 25 mol% did not affect the crystal structure and the phase composition of ferrite adsorbents.

Although no additional Cr-containing phase was detected, according to the surface atomic composition determined by EDS analysis (Table 2), Cr^{3+} ions were still present in $Co(Cr_{0.25}Fe_{0.75})_2O_4$ sample with the surface atomic content up to 6.38%. It should be reminded that the ionic radius of Cr^{3+} ions at octahedral sites is 0.615 Å [20], which is very close to that of Fe^{3+} ions (0.645 Å) at the octahedral sites of cubic spinel lattice [20].

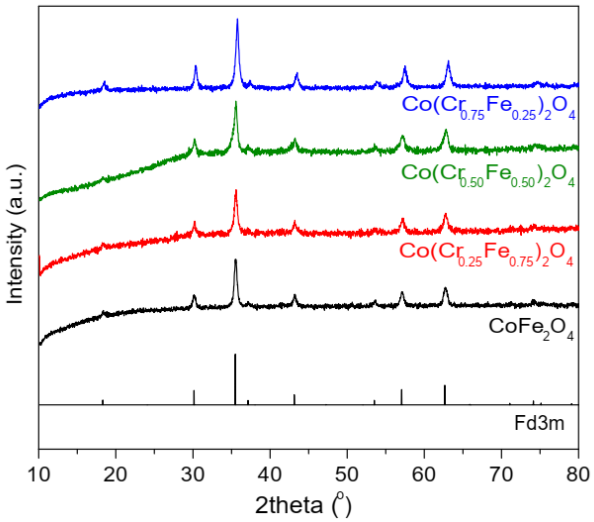

Fig. 2. XRD patterns of $CoFe_2O_4$, $Co(Cr_{0.25}Fe_{0.75})_2O_4$, $Co(Cr_{0.50}Fe_{0.50})_2O_4$ and $Co(Cr_{0.75}Fe_{0.25})_2O_4$ samples

This explained why Cr^{3+} ions can be substituted for Fe^{3+} ions in $CoFe_2O_4$ and why the formation of this solid solution is difficult to identify by XRD.

3.4. Morphology and specific surface area

The morphology of $CoFe_2O_4$ and $Co(Cr_{0.25}Fe_{0.75})_2O_4$ samples were investigated via their FE-SEM images. As shown in Fig. 3, both two samples consist of polyhedral particles with the particle size in the range of 30–50 nm. However, the particles of $CoFe_2O_4$ are found to be more strongly agglomerated than those of $Co(Cr_{0.25}Fe_{0.75})_2O_4$, which can be explained by the higher saturation magnetization of cobalt ferrite powders without Cr-substitution. Consequently, the $Co(Cr_{0.25}Fe_{0.75})_2O_4$ sample shows the enhanced

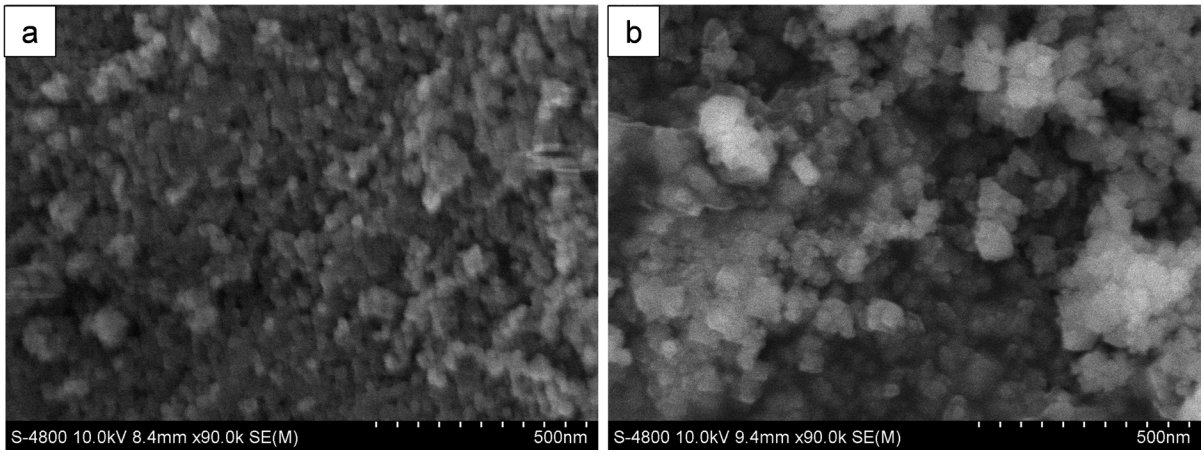

Fig. 3. FE-SEM images of $CoFe_2O_4$ (a) and $Co(Cr_{0.25}Fe_{0.75})_2O_4$ (b) samples

specific surface area (23.258 m^2/g^{-1}) whereas the specific surface area of $CoFe_2O_4$ is only 14.331 m^2/g^{-1} (Table 3).

Table 3. Specific surface area (S_{BET}) of $CoFe_2O_4$ and $Co(Cr_{0.25}Fe_{0.75})_2O_4$ samples

Ferrite	$CoFe_2O_4$	$Co(Cr_{0.25}Fe_{0.75})_2O_4$
S_{BET} (m^2 g^{-1})	14.331	23.258

3.5. Adsorption isotherms

The experimental dataset obtained from the study of phosphate adsorption isotherms for $CoFe_2O_4$ and $Co(Cr_{0.25}Fe_{0.75})_2O_4$ samples were fitted with the linear form by the Langmuir model (Fig. 4a) and Freundlich model (Fig. 4b). Then, their characteristic parameters were calculated and presented in Table 4. From the correlation coefficient R^2, it is noticed that all the adsorption isotherms are better described by the Langmuir model than Freundlich model. This result indicates that the precipitation of chromium phosphate or iron phosphate can be negligible [21] and the phosphate removal over our adsorbents follows the monolayer adsorption processes. Moreover, by using the Langmuir equation (Eq. 3), the adsorption rate constant of $Co(Cr_{0.25}Fe_{0.75})_2O_4$ sample was found to be 2.1160 $mgP.g^{-1}$, which is 4.85 times higher than $CoFe_2O_4$ (0.4365 mgP/g^{-1}).

3.6. Adsorption kinetics

In order to investigate the phosphate adsorption kinetics of $Co(Cr_xFe_{1-x})_2O_4$ samples, all kinetic data were fitted to the pseudo-first-order (Fig. 5a) and the pseudo-second-order (Fig. 5b). The calculated kinetic parameters were shown in Table 5. Owing to the higher correlation coefficients R^2, the pseudo-second-order model was proved to be more suitable for the phosphate adsorption on our materials. Accordingly, with the pseudo-second-order equation (Eq. 6), the phosphate adsorption rate constants of $CoFe_2O_4$ and $Co(Cr_{0.25}Fe_{0.75})_2O_4$ samples were estimated to be 0.4767 and 0.8106 $g/mgP^{-1}.min^{-1}$, respectively (Table 5), confirming that the phosphate adsorption process on our Cr-substituted sample is clearly faster than $CoFe_2O_4$.

3.7. Discussion

According to our experimental results, the chromium substitution at the level of 25 mol% did not only improve the maximal phosphate

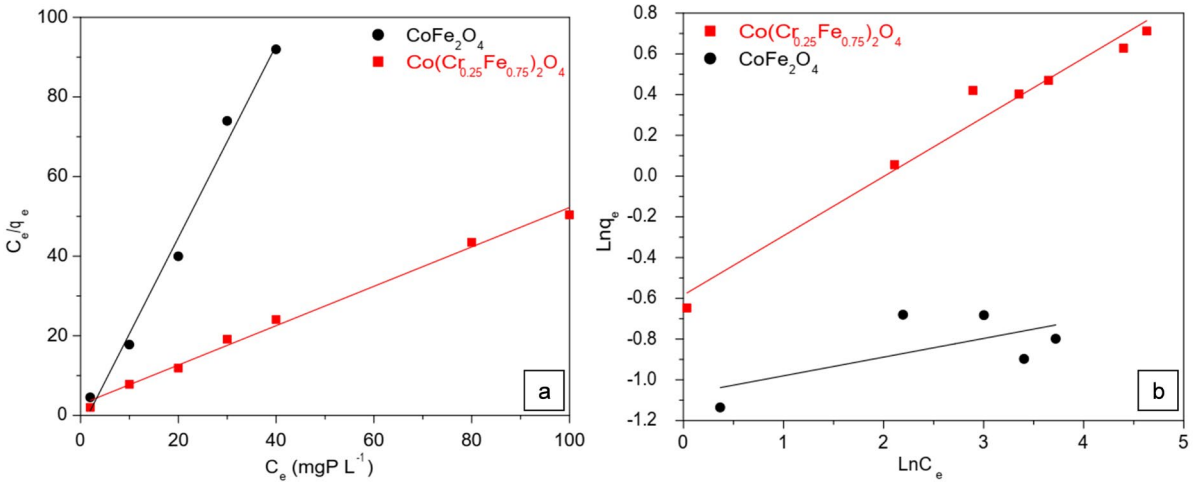

Fig. 4. F Linear fitting curves of C_e/q_e versus C_e for Langmuir model (a) and Lnq_e versus LnC_e for Freundlich model (b)

Table 4. Langmuir and Freundlich isotherm parameters for phosphate adsorption on $CoFe_2O_4$ and $Co(Cr_{0.25}Fe_{0.75})_2O_4$ samples

	Langmuir		Freundlich	
	q_m (mgP/g^{-1})	R^2	K_F (mgP/g^{-1})	R^2
$CoFe_2O_4$	0.4365	0.9864	0.3422	0.4243
$Co(Cr_{0.25}Fe_{0.75})_2O_4$	2.1160	0.9907	0.5576	0.9691

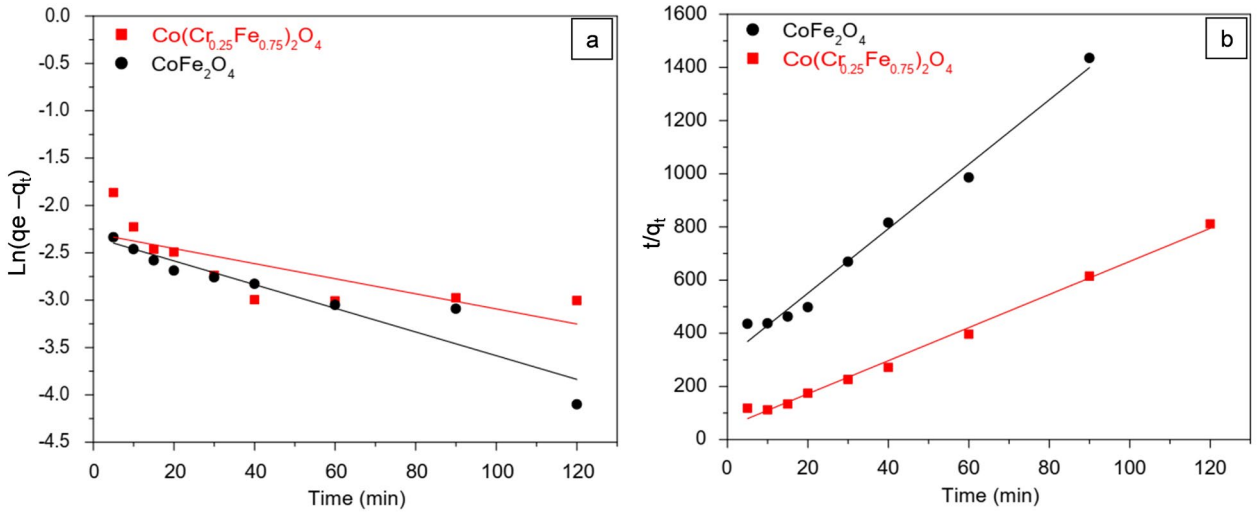

Fig. 5. Linear fitting curves of $Ln(q_e - q_t)$ versus time for pseudo-first-order model (a) and (t/q_t) versus time for pseudo-second-order model (b)

Table 5. Kinetic parameters of phosphate adsorption on $CoFe_2O_4$ and $Co(Cr_{0.25}Fe_{0.75})_2O_4$ samples

	Pseudo-first-order		Pseudo-second-order	
	k (min^{-1})	R^2	k (g mgP^{-1} min^{-1})	R^2
$CoFe_2O_4$	0.0086	0.8763	0.4767	0.9859
$Co(Cr_{0.25}Fe_{0.75})_2O_4$	0.0081	0.5791	0.8106	0.9933

adsorption capacity but also increased the phosphate adsorption rate of $CoFe_2O_4$ powders. This evolution should be assigned to the increase in surface specific area of Cr-substituted sample as well as the presence of Cr^{3+} species in the lattice and on the surface of magnetic powders. In fact, when Cr^{3+} ions ($x = 0.25$) were substituted for Fe^{3+} ions in $CoFe_2O_4$, the specific surface area was enhanced by the factor of 1.62, which can increase the number of adsorption sites for phosphate ions. Since the adsorption rate constant of $Co(Cr_{0.25}Fe_{0.75})_2O_4$ (k_2 = 0.8106 g/$mgP^{-1}.min^{-1}$) is also 1.70 times higher than that of $CoFe_2O_4$ (k_2 = 0.4767 g.$mgP^{-1}.min^{-1}$), we believe that the phosphate adsorption rate on our samples is strongly associated with their surface specific area. However, as mentioned in our isotherm study, when 25 mol% chromium was inserted to cobalt ferrite, the maximal adsorption capacity was greatly enhanced with the factor of 4.85, significantly outperforming the increase in surface specific area. Thus, in addition of large specific surface area, this enhancement of adsorption capacity should be attributed to the presence of Cr^{3+} species on the surface of $Co(Cr_{0.25}Fe_{0.75})_2O_4$ sample. In literature, the formation constant of $Cr(OH)_3H_2PO_4^-$ complex was reported to be $10^{2.78}$ [22] whereas that of $FeHPO_4^+$ complex is only $10^{1.28}$ [23]. Therefore, it is suggested that the existence of Cr(III) species on the ferrite surface can promote bonding with phosphate ions through complex formation, which improves the phosphate removal from solution.

4. Conclusions

Herein, the synthesis of chromium-substituted cobalt ferrite particles by a simple coprecipitation – annealing method and their application as novel magnetic adsorbents to the removal of phosphate ions from the solution were reported. All the Cr-substituted samples exhibited the enhanced adsorption toward phosphate ions in solution but their magnetic properties tend to decline with Cr content. Among our different samples, the 25 mol% Cr-substituted $CoFe_2O_4$ sample was considered as the most promising magnetic adsorbent since its saturation magnetization is still high enough for the quick separation from the solution by a magnet and its maximal phosphate adsorption capacity as well

as its phosphate adsorption rate constant are significantly superior to that of $CoFe_2O_4$, which can be attributed to the high surface specific area and the presence of Cr^{3+} species on the surface of Cr-substituted adsorbents.

Author contributions

The authors contributed equally to this article.

Conflict of interests

The authors declare that they have no known competing financial interests or personal relationships that could have influenced the work reported in this paper.

References

1. Cooperband L. R., Good L. W. Biogenic phosphate minerals in manure: implications for phosphorus loss to surface waters. *Environmental Science & Technology*. 2002;36(23): 5075–5082. https://doi.org/10.1021/es025755f

2. Oguz E., Gurses A., Canpolat N. Removal of phosphate from wastewaters. *Cement and Concrete Research*. 2003;33(8): 1109–1112. https://doi.org/10.1016/S0008-8846(03)00016-4

3. Smith V. H., Schindler D. W. Eutrophication science: where do we go from here? *Trends in Ecology & Evolution*. 2009;24(4): 201–207. https://doi.org/10.1016/j.tree.2008.11.009

4. Guo H., Li W., Wang H., Zhang J., Liu Y., Zhou Y. A study of phosphate adsorption by different temperature treated hydrous cerium oxides. *Rare Metals*. 2011;30: 58–62. https://doi.org/10.1007/s12598-011-0197-5

5. Cheng X., Huang X., Wang X., Sun D. J. Influence of calcination on the adsorptive removal of phosphate by Zn–Al layered double hydroxides from excess sludge liquor. *Journal of Hazardous Materials*. 2010;177: 516–523. https://doi.org/10.1016/j.jhazmat.2009.12.063

6. Lu S. G., Bai S. Q., Zhu L., Shan H. D. Removal mechanism of phosphate from aqueous solution by fly ash. *Journal of Hazardous Materials*. 2009;161: 95–101. https://doi.org/10.1016/j.jhazmat.2008.02.123

7. Delaneya P., Manamon C. M., Hanrahan J. P., Copley M. P., Holmes J. D., Morris M. A. Development of chemically engineered porous metal oxides for phosphate removal. *Journal of Hazardous Materials*. 2011;185: 382–391. https://doi.org/10.1016/j.jhazmat.2010.08.128

8. Zhang X., Sun F., He J., Xu H., Cui F., Wang W. Robust phosphate capture over inorganic adsorbents derived from lanthanum metal organic frameworks. *Chemical Engineering Journal*. 2017;326: 1086–1094. https://doi.org/10.1016/j.cej.2017.06.052

9. Santos L. C., da Silva A. F., dos Santos Lins P. V., da Silva Duarte J. L., Ide A. H., Meili L. Mg-Fe layered double hydroxide with chloride intercalated: Synthesis, characterization and application for efficient nitrate removal. *Environmental Science and Pollution Research*. 2020;*27*: 5890–5900. https://doi.org/10.1007/s11356-019-07364-4

10. Sunday K. J., Taheri M. L. NiZnCu-ferrite coated iron powder for soft magnetic composite applications. *Journal of Magnetism and Magnetic Materials*. 2018;463: 1–6. https://doi.org/10.1016/j.jmmm.2018.05.030

11. Anupama A. V., Kumaran V., Sahoo B. Application of Ni-Zn ferrite powders with polydisperse spherical particles in magnetorheological fluids. *Powder Technology*. 2018;338: 190–196. https://doi.org/10.1016/j.powtec.2018.07.008

12. Hoang N. T. P., Le T. K. Polyethylene glycol-assisted sol-gel synthesis of magnetic $CoFe_2O_4$ powder as photo-Fenton catalysts in the presence of oxalic acid. *Journal of Sol-Gel Science and Technology*. 2018;88: 211–219. https://doi.org/10.1007/s10971-018-4783-y

13. Lai L., Xie Q., Chi L., Gu W., Wu D. Adsorption of phosphate from water by easily separable Fe_3O_4@SiO_2 core/shell magnetic nanoparticles functionalized with hydrous lanthanum oxide. *Journal of Colloid and Interface Science*. 2016;465: 76–82. https://doi.org/10.1016/j.jcis.2015.11.043

14. Lin Z, Chen J. Magnetic Fe_3O_4@MgAl-LDH@$La(OH)_3$ composites with a hierarchical core-shell structure for phosphate removal from wastewater and inhibition of labile sedimentary phosphorus release. *Chemosphere*. 2021; 264: 128551. https://doi.org/10.1016/j.chemosphere.2020.128551

15. APHA (American Public Health Association). Standard methods for the examination of water and wastewater, 19th ed. *APHA*, Washington, DC. 1995.

16. Raghasudha M., Ravinder D., Veerasomaiah P. Magnetic properties of Cr-substituted Co-ferrite nanoparticles synthesized by citrate-gel autocombustion method. *Journal of Nanostructure in Chemistry*. 2013;3: 63. https://doi.org/10.1186/2193-8865-3-63

17. Li Z., Dai J., Cheng C., Suo Z., quing W. Synthesis and magnetic properties of chromium doped cobalt ferrite nanotubes. *Materials Research Express*. 2020;7: 086102. https://doi.org/10.1088/2053-1591/abae26

18. Fournier J. T., Landry R. J. ESR of Exchange coupled Cr^{3+} ions in phosphate glass. *The Journal of Chemical Physics*. 1971;55: 2522–2525. https://doi.org/10.1063/1.1676442

19. Worsztynowicza A., Kaczmareka S. M., Kurzawab M., Bosacka M. Magnetic study of Cr^{3+} ion in $M_2CrV_3O_{11-x}$ (M=Zn, Mg) compounds. *Journal of Solid State Chemistry*. 2005;178: 2231–2236. https://doi.org/10.1016/j.jssc.2005.04.033

20. Shannon R. D. Revised effective ionic radii and systematic studies of interatomic distances in halides

and chalcogenides. *Acta Crystallographica Section A*. 1976;32: 751–767. https://doi.org/10.1107/S0567739476001551

21. Del Bubba M., Arias C. A., Brix H. Phosphorus adsorption maximum of sands for use as media in subsurface flow constructed reed beds as measured by the Langmuir isotherm, *Water Research*. 2003;37: 3390–3400. https://doi.org/10.1016/S0043-1354(03)00231-8

22. Rai D., Moore D. A., Hess N. J., Rao L., Clark S. B. Chromium(III) hydroxide solubility in the aqueous $Na^+–OH^-–H_2PO_4^-–HPO_4^{2-}–PO_4^{3-}–H_2O$ system: a thermodynamic model. *Journal of Solution Chemistry*. 2007;36: 1213–1242. https://doi.org/10.1007/s10953-007-9179-5

23. Lente G., Magalhães M. E. A., Fábián. I. Kinetics and mechanism of complex formation reactions in the iron(III)-phosphate ion system at large iron(III) excess. Formation of a tetranuclear complex. *Inorganic Chemistry*. 2000;39: 1950–1954. https://doi.org/10.1021/ic991017p

Information about the authors

Qui Anh Tran, 4th year student, Faculty of Chemistry, University of Science, Vietnam National University (Ho Chi Minh City, Vietnam).
trananh370@gmail.com
https://orcid.org/0000-0002-0365-8794

Nhat Linh Tran, 4th year student, Faculty of Chemistry, University of Science, Vietnam National University (Ho Chi Minh City, Vietnam).
tnllinh95@gmail.com
https://orcid.org/0000-0001-8527-1958

Dang Khoa Nguyen Anh, 3rd year student, Faculty of Chemistry, University of Science, Vietnam National University (Ho Chi Minh City, Vietnam).
nguyenkhoa260701@gmail.com
https://orcid.org/0000-0002-0968-0968

Quynh Nhu Le Thi, 3rd year student, Faculty of Chemistry, University of Science, Vietnam National University (Ho Chi Minh City, Vietnam).
ltqnhu2608@gmail.com
https://orcid.org/0000-0002-8081-5570

The Luan Nguyen, Master in Chemistry, Faculty of Chemistry, University of Science, Vietnam National University (Ho Chi Minh City, Vietnam).
ntluan@hcmus.edu.vn
https://orcid.org/0000-0001-6305-6878

Huu Thinh Pham Nguyen, Master in Chemistry, Faculty of Chemistry, University of Science, Vietnam National University (Ho Chi Minh City, Vietnam).
pnhthinh@hcmus.edu.vn
https://orcid.org/0000-0002-9308-5263

Anh Tien Nguyen, PhD in Chemistry, Chief of Inorganic Chemistry Department, Ho Chi Minh City University of Education (Ho Chi Minh City, Vietnam).
tienna@hcmue.edu.vn
https://orcid.org/0000-0002-4396-0349

Quoc Thiet Nguyen, PhD in Chemistry, Institute of Applied Materials Science, Vietnam Academy of Science and Technology (Ho Chi Minh City, Vietnam).
ngqthiet@yahoo.com
https://orcid.org/0000-0002-2218-9225

Tien Khoa Le, PhD in Chemistry, Chief of Inorganic Chemistry Department, University of Science, Vietnam National University (Ho Chi Minh City, Vietnam).
ltkhoa@hcmus.edu.vn
https://orcid.org/0000-0003-0058-0298

Received 29.03.2022; approved after reviewing 06.06.2022; accepted for publication 15.07.2022; published online 25.09.2022.